Tellus
SERIES B
CHEMICAL
AND PHYSICAL
METEOROLOGY
PUBLISHED BY THE INTERNATIONAL METEOROLOGICAL INSTITUTE IN STOCKHOLM

Tellus (2010), 62B, 729–742

Evaluation of a terrestrial carbon cycle submodel in an Earth system model using networks of eddy covariance observations

By TAKASHI SUZUKI* and KAZUHITO ICHII, *Faculty of Symbiotic Systems Science, Fukushima University, 1 Kanayagawa, Fukushima 960–1296, Japan*

(Manuscript received 30 December 2009; in final form 14 June 2010)

ABSTRACT

Improvement of terrestrial submodels in Earth system models (ESMs) is important to reduce uncertainties in future projections of global carbon cycle and climate. Since these submodels lack detailed validation, evaluation of terrestrial submodels using networks of field observations is necessary. The purpose of this study is to improve an ESM by refining a terrestrial submodel using eddy covariance observations. We evaluated the terrestrial submodel (MOSES2/TRIFFID) included in the UVic Earth System Climate Model (UVic-ESCM) and tested the effects of terrestrial submodel improvements on future projection of carbon cycle and climate. First, we evaluated the terrestrial submodel as an off-line mode at point scales using 48 eddy covariance observation data, and improved it through fixing model parameters and structures. The terrestrial submodel was improved with the reduction of the root mean square error and the closer simulation of the seasonal carbon fluxes. Second, using the UVic-ESCM with the improved terrestrial submodel, we confirmed model improvement at most observation sites. The terrestrial submodel refinement also affected future projections; the UVic-ESCM with the improved terrestrial submodel simulated 100 ppmv lower atmospheric CO_2 concentration in 2100 compared with the default UVic-ESCM. Our study underscores the importance of refinement of terrestrial submodels in ESM simulations.

1. Introduction

Earth system models (ESMs), which simulate the coupled cycle of climate and carbon among the atmosphere, land, and ocean, are now widely used to project future changes in climate and carbon cycle due to anthropogenic CO_2 emission (e.g. Cox et al., 2000; Lenton, 2000; Joos et al., 2001; Dufresne et al., 2002; Ichii et al., 2003; Kheshgi and Jain, 2003; Zeng et al., 2004; Friedlingstein et al., 2006). The inclusion of coupled climate-carbon cycle causes a positive climate-carbon cycle feedback effect and amplifies future climate changes on both global and regional scales (e.g. Cox et al., 2000; Friedlingstein et al., 2006; Yoshikawa et al., 2008). These ESMs have also been used to simulate historical changes in the global carbon cycle (e.g. Kato et al., 2009), to analyse the future CO_2 emission targets in an effort to stabilize the atmospheric CO_2 concentration (e.g. Matthews et al., 2005a; Miyama and Kawamiya, 2009; Zickfeld et al., 2009) and to determine the effectiveness of geoengineering schemes (Matthews and Caldeira, 2008).

*Corresponding author.
e-mail: s0970031@ipc.fukushima-u.ac.jp
DOI: 10.1111/j.1600-0889.2010.00478.x

These ESMs contain large uncertainties among models (Friedlingstein et al., 2006) and need further improvements. Through the model intercomparison study, Friedlingstein et al. (2006) pointed out that the uncertainty of the carbon budget and its feedback effects for in the terrestrial biosphere is larger than those reported for in the ocean. For example, they demonstrated that the projected terrestrial carbon budget differs among models even in sign. Therefore, further improvement of terrestrial submodels is required. One of the potential causes of the uncertainties is inaccurate parametrizations of various subprocesses. Therefore, more evaluation and calibration of model are required using observation.

Focusing on the terrestrial submodels as carbon cycle and climate off-line modelling, many studies have evaluated performance of terrestrial submodels using ground and/or satellite observations (e.g. Medlyn et al., 2005; Morales et al., 2005; Kucharik et al., 2006; Siqueira et al., 2006; Abramowitz et al., 2008; Randerson et al., 2009; Mahecha et al., 2010; Zaehle and Friend, 2010). These works evaluated terrestrial submodels at multiple eddy covariance sites (e.g. Morales et al., 2005; Kucharik et al., 2006; Zaehle and Friend, 2010), and developed effective methods for model-data evaluations (e.g. Medlyn et al., 2005; Kucharik et al., 2006; Siqueira et al., 2006; Abramowitz

et al., 2008; Randerson et al., 2009; Mahecha et al., 2010). These model evaluations and improvements need to be analysed within the ESM framework.

Furthermore, many studies have analysed the effects of the uncertainties in the terrestrial submodels on future climate and carbon cycle projection within the ESM framework (e.g. Ichii et al., 2003; Jones et al., 2003; Thompson et al., 2004; Matthews et al., 2005a; Bala et al., 2006; O'Ishi et al., 2009). Jones et al. (2003) analysed the effect of different temperature sensitivities of soil decomposition. Thompson et al. (2004), Matthews et al. (2005a), and Bala et al. (2006) analysed the impact of the setting of the photosynthesis model on future projections. O'Ishi and Abe-Ouchi (2009) tested the impact of biogeographical, biogeochemical and biogeophysical effects under quadrupled CO_2 concentrations. Most of these analyses lack validations of terrestrial submodels. As one exception, Kato et al. (2009) evaluated the seasonality and interannual variabilities of terrestrial carbon fluxes. They found that only four of fifteen validation sites simulated reasonable seasonal and interannual variation of Net Ecosystem Productivity (NEP). Therefore, we need to improve the terrestrial submodel in ESM, and analyse the effects of site level performance evaluations and corresponding model improvements to a fully coupled ESM.

Eddy covariance observation data have become widely available in recent years (e.g. Baldocchi et al., 2001; Baldocchi, 2008), and these data can be used to evaluate and refine ESMs. Thus, in this study, we evaluated and improved a terrestrial submodel included in an ESM using about 50 eddy covariance observations. Then, we evaluated the effects of improvement of the terrestrial submodel on future projections of global environmental changes based on an ESM. Toward a systematic method of refining ESMs, which is also applicable to other ESMs, we first conducted an off-line model experiment and improved the terrestrial submodel alone. Then, by connecting back to the ESM, we assessed the effect of terrestrial submodel improvements on the ESM simulations at both point and global scales.

2. Model and data

2.1. Model

2.1.1. Earth system model. We used the University of Victoria Earth System Climate Model (UVic-ESCM) version 2.8 (Weaver et al., 2001; Matthews et al., 2009; Zickfeld et al., 2009). The UVic-ESCM is an ESM of intermediate complexity that includes coupled processes of climate and carbon cycle among atmosphere, land and ocean. The model consists of a vertically integrated energy–moisture balance atmospheric model coupled to the Modular Ocean Model version 2 (MOM2) ocean general circulation model (Pacanowski, 1995), terrestrial and ocean carbon cycle model, and a dynamic–thermodynamic seaice model (Bitz et al., 2001). The terrestrial submodel consists of a modified version of a simple land surface model, Met Office Surface Exchange Scheme version 2 (MOSES2; Essery and Clark, 2003), and a dynamic vegetation model, Top-down Representation of Interactive Foliage and Flora including Dynamics (TRIFFID; Cox, 2001) (Meissner et al., 2003). The horizontal resolution is $1.8^\circ \times 3.6^\circ$, and the ocean model has 19 vertical levels. The model has been widely used to project future global environmental changes due to anthropogenic CO_2 emission (Matthews et al., 2005b) and inversely calculate allowable anthropogenic CO_2 emission (Matthews and Caldeira, 2008). Details of the terrestrial submodel are given in the next section.

2.1.2. Terrestrial submodel. A coupled model of MOSES2 and TRIFFID (MOSES2/TRIFFID) simulates carbon and water fluxes, such as photosynthesis and evapotranspiration, at an hourly time scale for vegetation and soil. It defines five plant functional types (PFTs): broadleaf tree, needleleaf tree, C3 grass, C4 grass and shrubs. Photosynthesis is calculated by a function of CO_2, light, soil moisture, temperature and nutrients using a leaf-level model (Collatz et al., 1991, 1992) with coupled photosynthesis and stomatal conductance (Cox et al., 1999). Using the accumulated carbon fluxes passed from MOSES2, TRIFFID updates the vegetation and soil carbon at a monthly time scale. The vegetation dynamics module in TRIFFID also updates the fraction of each PFT based on the Lotka-Volterra competition equations. Carbon is passed to a single soil carbon pool through litterfall and vegetation mortality. Soil carbon decomposition is controlled by soil temperature using a Q_{10} formulation and water stress.

The MOSES2/TRIFFID model was modified to suit simplicity of the UVic-ESCM. The MOSES2 is slightly different from its original version (Meissner et al., 2003) in its algorithm and structure. Difference are that soil water box is set as one box, rooting depths are set constant for all vegetation types (default: 1 m), and canopy interception of rainfall and its evaporation are not considered. The TRIFFID model is the same as the original one (Cox, 2001) except for some slightly different parameter settings.

The required model climate inputs are as follows: daily climate of average temperature (Tave), precipitation (Prec), relative humidity (RH), incoming surface solar radiation (Srad), diurnal temperature range (DTR) and wind speed (Wind). Atmospheric CO_2 concentration is also necessary to run the model. For the off-line simulation (see Section 3.1), we extracted the terrestrial submodel from UVic-ESCM to run the model in off-line mode forced by external climate data as model inputs. In the ESM simulation (see Section 3.2), these time variables for the model inputs are passed by the atmospheric submodel.

2.2. Site observation data

We used data from 48 eddy covariance observation sites across Ameriflux, CarboEurope and AsiaFlux to evaluate the terrestrial submodel. To select sites, we used the sites that have less missing data in the time series. Details for each site

Table 1. Flux observation sites used in this study

Site name	Short ID	Country	Longitude	Latitude	Veg. type	Year	References
Bartlett Experimental Forest	USBar	US	71°17′W	44°04′N	DBF	2005	Jenkins et al. (2007)
Blodgett Forest	USBlo	US	120°38′W	38°54′N	ENF	2000–2005	Goldstein et al. (2000) Misson et al. (2006)
Brookings	USBkg	US	96°50′W	44°21′N	GL	2005–2006	Gilmanov et al. (2005)
Donaldson	USSP3	US	82°10′W	29°45′N	ENF	1999–2004	Powell et al. (2008)
Fermi Prairie	USIB2	US	88°14′W	41°50′N	GL	2005–2006	–
Fort Peck	USFPe	US	105°06′W	48°18′N	GL	2000–2006	–
Goodwin Creek	USGoo	US	89°58′W	34°15′N	CR	2004–2006	–
Harvard Forest	USHa1	US	72°10′W	42°32′N	DBF	1996–2006	Wofsy et al. (1993)
Howland Forest Main	USHo1	US	68°44′W	45°12′N	MF	1996–2004	Hollinger et al. (1999, 2004)
Howland Forest West Tower	USHo2	US	68°44′W	45°13′N	MF	1999–2004	Hollinger et al. (1999, 2004)
Metolius New Young Pine	USMe3	US	121°34′W	44°26′N	ENF	2004–2005	Hollinger et al. (1999, 2004)
Metolius Old Pine	USMe4	US	121°37′W	44°30′N	ENF	1997–2000	Law et al. (2003, 2004) Irvine et al. (2007)
Missouri Ozark	USMOz	US	92°12′W	38°45′N	EBF	2005–2006	Gu et al. (2006, 2007)
Mize	USSP2	US	82°15′W	29°46′N	ENF	2000–2004	–
Morgan Monroe State Forest	USMMS	US	86°25′W	39°19′N	DBF	1999–2005	Schmid et al. (2000)
North Carolina Loblolly Pine	USNC2	US	76°40′W	36°48′N	MF	2005–2006	Oren et al. (1998, 2006)
Tonzi Ranch	USTon	US	120°58′W	38°26′N	WS	2002–2006	Baldocchi et al. (2004)
UMBS Univ Michigan	USUMB	US	84°43′W	45°34′N	MF	2000–2003	Gough et al. (2008)
Vaira Ranch	USVar	US	120°57′W	38°24′N	WS	2002–2006	Ma et al. (2007) Baldocchi et al. (2004)
UCI 1850	CANS1	CA	98°29′W	55°53′N	ENF	2003–2004	McMillan et al. (2008)
UCI 1930	CANS2	CA	98°31′W	55°54′N	ENF	2003	McMillan et al. (2008)
UCI 1964	CANS3	CA	98°23′W	55°55′N	ENF	2002–2004	McMillan et al. (2008)
UCI 1964wet	CANS4	CA	98°23′W	55°55′N	ENF	2003	McMillan et al. (2008)
UCI 1981	CANS5	CA	98°29′W	55°52′N	ENF	2003–2004	McMillan et al. (2008)
UCI 1989	CANS6	CA	98°58′W	55°55′N	ENF	2002–2004	McMillan et al. (2008)
UCI 1998	CANS7	CA	99°57′W	56°38′N	ENF	2003–2004	McMillan et al. (2008)
Tapajos KM67	BRSa1	BR	54°58′W	2°51′S	EBF	2002–2004	Saleska et al. (2003) Hutyra et al. (2007)
Tapajos KM83	BRSa3	BR	54°58′W	3°01′S	EBF	2001–2003	Goulden et al. (2004)
Amplero	ITAmp	IT	13°36′E	41°54′N	GL	2004	–
Bugac	HUBug	HU	19°36′E	41°42′N	GL	2005	–
Collelongo	ITCol	IT	13°35′E	41°51′N	DBF	1998	Van Dijk and Dolman (2004)
Hainich	DEHai	DE	10°27′E	51°05′N	DBF	2000–2003	Knohl et al. (2003)
Hesse	FRHes	FR	7°04′E	48°40′N	DBF	1998–2003	Granier et al. (2000)
Hyyti	FIHyy	FI	24°18′E	61°51′N	ENF	1999–2005	Rannik et al. (2004)
Loobos	NLLoo	NL	5°45′E	52°10′N	ENF	1997–2004	Van Dijk and Dolman (2004)
Nonantola	ITNon	IT	11°05′E	44°41′N	MF	2001–2002	Reichstein et al. (2005)
Parco_Ticino_forest	ITPT1	IT	9°04′E	45°12′N	ENF	2003	–
Roccarespampani 2	ITRo2	IT	11°55′E	42°23′N	DBF	2002–2004	Kowalski et al. (2004)
San_Rossore	ITSRo	IT	10°17′E	43°44′N	ENF	2003	Reichstein et al. (2005)
Sodankylä	FISod	FI	26°38′E	67°22′N	ENF	2003–2005	Tanja et al. (2003)
Soroe	DKSor	DK	11°39′E	55°29′N	MF	1998–2003	Pilegaard et al. (2001)
Tharandt	DETha	DE	13°34′E	50°58′N	ENF	2000–2003	Van Dijk and Dolman (2004)
Vielsalm	BEVie	BE	5°60′E	50°18′N	MF	1999–2001	Aubinet et al. (2001)

are given in Table 1. All data of meteorological observations and carbon and water flux observations are gap-filled and flux-partitioned [e.g. NEP into Gross Primary Productivity (GPP) and Ecosystem Respiration (RE)]. We used the Level 4 eddy covariance observation standardized datasets provided by Ameriflux (http://public.ornl.gov/ameriflux) and CarboEurope (http://www.carboeurope.org). As the carbon fluxes, we used average of the estimations from different gap-filling methods (ar-

Table 1. Continued

Site name	Short ID	Country	Longitude	Latitude	Veg. type	Year	References
Wetzstein	DEWet	DE	11°27′E	50°27′N	ENF	2004–2005	Anthoni et al. (2004)
Maeklong	THMek	TH	98°51′E	14°35′N	DBF	2003–2004	Saigusa et al. (2008)
Southern Khentei Taiga	MNSkt	MN	108°39′E	48°21′N	DNF	2004–2005	Li et al. (2005)
Takayama	JPTak	JP	137°25′E	36°09′N	DBF	2001–2004	Saigusa et al. (2002)
Tomakomai	JPTom	JP	141°31′E	42°44′N	DNF	2001–2003	Hirata et al. (2007)

Notes: Abbreviations for country: United States (US), Canada (CA), Brazil (BR), Italy (IT), Hungary (HU), Germany (DE), France (FR), Finland (FI), Netherlands (NL), Denmark (DK), Belgium (BE), Thailand (TH), Mongolia (MN) and Japan (JP).
Abbreviations for vegetation type: Evergreen Needleleaf Forest (ENF), Evergreen Broadleaf Forest (EBF), Deciduous Needleleaf Forest (DNF), Deciduous Broadleaf Forest (DBF), Mixed Forest (MF), Grassland (GL), Shrubland (SH) and Cropland (CR).

tificial neural network and marginal distribution sampling techniques; Papale and Valentini 2003; Reichstein et al., 2005; Moffat et al., 2007). Asiaflux data are gap-filled and flux-partitioned based on Hirata et al. (2008) and Saigusa et al. (2008). Monthly averages of the water and carbon fluxes [evapotranspiration (ET), GPP, RE and NEP] were calculated for model validation.

From meteorological observations at eddy covariance observation sites, we also created the climate input data (Tave, Prec, RH, Srad, DTR and Wind) for the MOSES2/TRIFFID model. For off-line simulation, we used observed climate data from each eddy covariance observation site and long-term climate reanalysis data (1948–2006) from NCEP/NCAR reanalysis data (Kalnay et al., 1996), which was extracted at the corresponding grid. NCEP/NCAR reanalysis data were used to extend period of observed climate data at each site because observational period of these data were short. For Tave and Srad, NCEP/NCAR reanalysis data were corrected using observed daily data based on linear regression. For Prec, daily NCEP/NCAR precipitation data were corrected using observed monthly total precipitation data by obtaining the multiplier while preserving the frequency of rainy days of NCEP/NCAR reanalysis data. For other climate input data, we used NCEP/NCAR reanalysis data directly.

3. Experiments

To evaluate and improve the terrestrial submodel included in the UVic-ESCM, we conducted two experiments: an off-line experiment and an ESM experiment (Fig. 1). In the off-line experiment, we used the terrestrial submodel forced by observed climate inputs (off-line model run). We evaluated and refined the model at a point scale using eddy covariance observations. In this process, we first tested the default MOSES2/TRIFFID model with eddy covariance observations (default MOSES2/TRIFFID). Next, we refined the MOSES2/TRIFFID model using eddy covariance observations (improved MOSES2/TRIFFID). Then, in the ESM experiment (carbon cycle-climate coupled model run), we used the default and improved MOSES2/TRIFFID model as a terrestrial submodel in the UVic-ESCM. We tested the effects of the terrestrial submodel improvements on the ESM simulations.

3.1. Off-line experiments

We conducted off-line simulations using the terrestrial submodel extracted from UVic-ESCM (Step 1 in Fig. 1). We ran the submodel with the default settings at each eddy covariance observation site using input climate data. Then, we tuned the submodel and its parameters to reproduce the observed ET, GPP, RE and NEP. Spin-up was conducted using whole 1948–2006 climate data with the atmospheric CO_2 concentration fixed at the 1948 level (310.3 ppmv) for 1000 yr. After that, we ran the model from 1948 to 2006 with a time-variant CO_2 concentration (Etheridge et al., 1998; Keeling et al., 2009).

Evaluation of the terrestrial submodel was conducted by comparing with observed ET, GPP, RE, and NEP at monthly temporal scales. To highlight the effect of the model improvement on outputs, we analysed the results from both the default and improved models with observations. Then, we discussed how the model improvements were effective and which processes have potential problems in the default model. First, we evaluated the modelled ET, GPP, RE, and NEP at all sites, by comparing with observed data at a monthly time scale. Second, to investigate in more detail, the seasonal time series in ET, GPP, RE and NEP were evaluated at each eddy covariance observation site. To analyse the effect of the model refinement, we calculated the root mean square error (RMSE) between observed and modelled monthly variations in ET, GPP, RE and NEP from the default and improved models, respectively.

3.2. ESM experiments

Using the UVic-ESCM with the default and improved terrestrial submodels, we conducted a two-step ESM experiment to analyse the effect of the terrestrial submodel improvement on the future projection of the global carbon cycle and climate. First, we evaluated the modelled carbon (GPP, RE and NEP) and water (ET) fluxes at eddy covariance observation sites (Step 2 in Fig. 1). We evaluated the monthly variations in carbon and water fluxes extracted from the corresponding grid, with the same eddy covariance observation sites as in the off-line experiment. Second, we analysed the effect of the terrestrial submodel

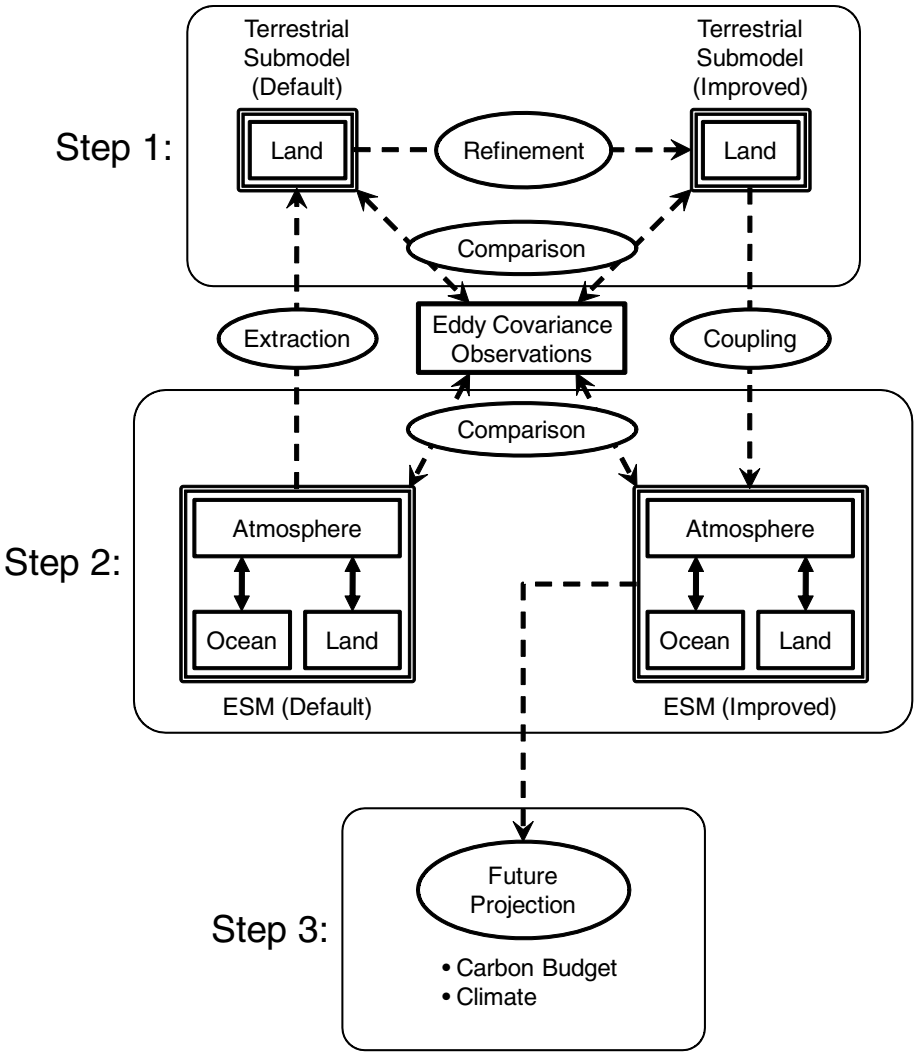

Fig. 1. Overview of the procedure of the ESM improvement in this study. In step 1, we extracted the terrestrial submodel (MOSES2/TRIFFID) from the UVic-ESCM, and we evaluated and refined it using eddy covariance observations. In step 2, we evaluated the effect of terrestrial submodel improvements on the ESM simulation at the eddy covariance observation site. In step 3, we evaluated the effect of terrestrial submodel improvements on the projection of the carbon cycle and climate based on the ESM simulation at a global scale.

refinement on the future projection of the global carbon cycle and climate changes (Step 3 in Fig. 1). By running UVic-ESCM with the default and improved terrestrial submodels until 2100, we evaluated the differences in the global carbon budget [atmospheric CO_2 concentration, terrestrial carbon fluxes and pools (GPP, NEP, biomass and soil carbon pools)] and temperature between these two different ESM settings.

The model spin-up and run includes three steps: uncoupled and coupled model spin-up, and coupled model run. First, with CO_2 concentration fixed at the 1850 level, uncoupled spin-up was conducted for 500 yr. Second, coupled spin-up was conducted for another 500 yr. Then, we ran the model from 1850 to 2100 using historical CO_2 emission (Marland et al., 2005) and the Intergovernmental Panel on Climate Change (IPCC) Special Report on Emissions Scenarios (SRES) A2 emission scenario.

4. Results

4.1. Off-line experiments

In the default terrestrial submodel simulation, the model overall underestimated observed monthly ET and carbon fluxes (GPP, RE and NEP) (Fig. 2) as a result of all sites comparison. The slopes of the regression lines deviated largely from 1.0 (0.52, 0.36, 0.48 and 0.02 for ET, GPP, RE and NEP, respectively) and correlation between observation and model was moderate except for NEP ($R^2 = 0.57$, 0.64, 0.69 and 0.00 for ET, GPP, RE and

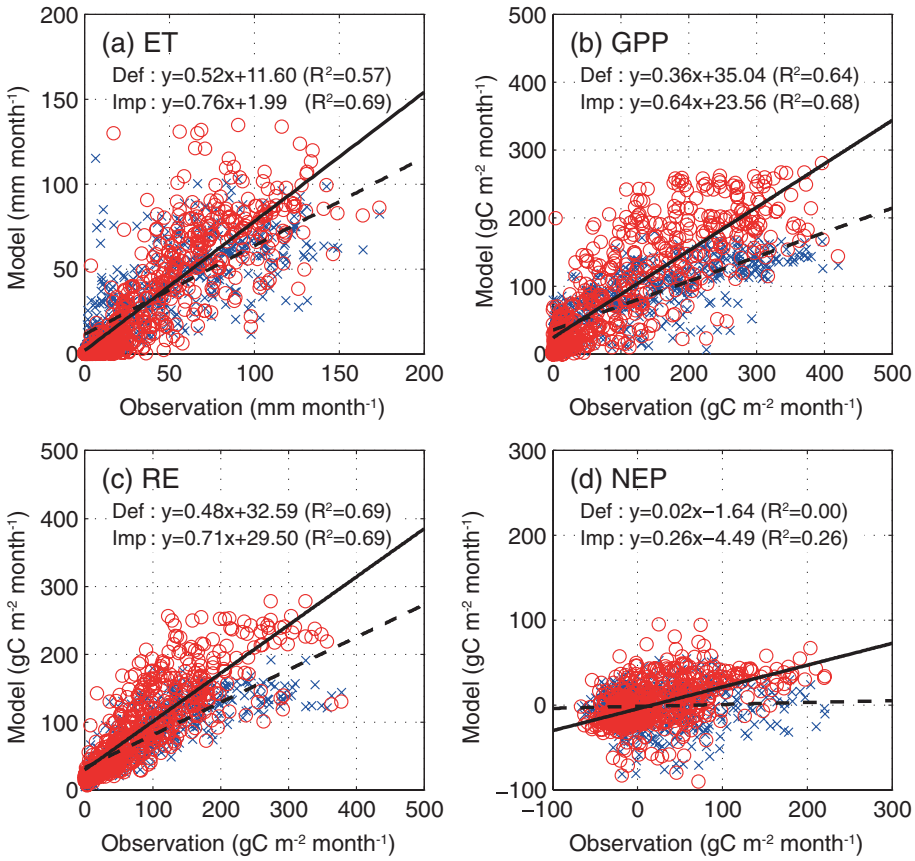

Fig. 2. Observed and modelled (default (blue) and improved (red) terrestrial submodels in the off-line experiment) monthly variations in (a) ET, (b) GPP, (c) RE and (d) NEP for all sites.

NEP, respectively). Of note, there was no correlation between modelled and observed NEP; the terrestrial submodel failed to reproduce observed NEP.

To investigate this issue in more detail, monthly variation in ET and carbon fluxes (GPP, RE and NEP) at four representative sites from different climatic zones (Hyyti, Finland (FIHyy) as a high latitude site; Howland Forest, US (USHo2) as a mid-latitude site; Takayama, Japan (JPTak) as a mid-latitude site and Tapajos KM67, Brazil (BRSa1) as a tropical site) were investigated (Fig. 3). We found that simulated seasonal variation of water and carbon fluxes largely deviated from the observations for all sites. For example, for ET, all sites underestimated its seasonal peak (Figs 3a, e, i and m). In USHo2 and JPTak, ET was overestimated during the snow season in winter and spring (Figs 3e and i) due to overestimation of snow sublimation. For GPP and RE, most sites underestimated their seasonal amplitude (i.e. the peak magnitudes in summer). In USHo2 and JPTak, simulated seasonal peak of GPP was substantially lower than observed peaks (Figs 3b, c, f, g, j, k, n and o). Nevertheless, simulated GPP was overestimated during spring and autumn (Figs 3f and j). In BRSa1, both GPP and RE were underestimated by half of the observed value with a GPP decline during the dry season (from August to November in this site), which is inconsistent with observations (Figs 3n and o). The model also failed to reproduce the NEP seasonal phase as well as amplitude (Figs 3d, h, l and p). The major cause is substantial underestimation of simulated GPP compared with RE. In FIHyy, seasonal variation pattern of NEP was comparatively well reproduced; however, the peaks were underestimated (Fig. 3d). In USHo2, JPTak and BRSa1, NEP seasonal variations were not reproduced with negative land carbon uptake during summer (USHo2 and JPTak) and the dry season (BRSa1) (Figs 3h, l and p).

Through the default submodel simulation, we found that the default terrestrial submodel needs substantial refinements to reproduce carbon and water fluxes more accurately. To improve the terrestrial submodel, we set the following guideline to minimize the ambiguity and subjectivity of the model modification. First, we used the slopes of regression lines and determination coefficients between observed and simulated seasonal water and carbon cycles as criteria for model evaluation. We modified the terrestrial submodel to bring the slopes of regression lines and determination coefficients closer to 1. Second, only the minimum changes were applied to the model. Through the sensitive analysis of various model parameters, a few influential

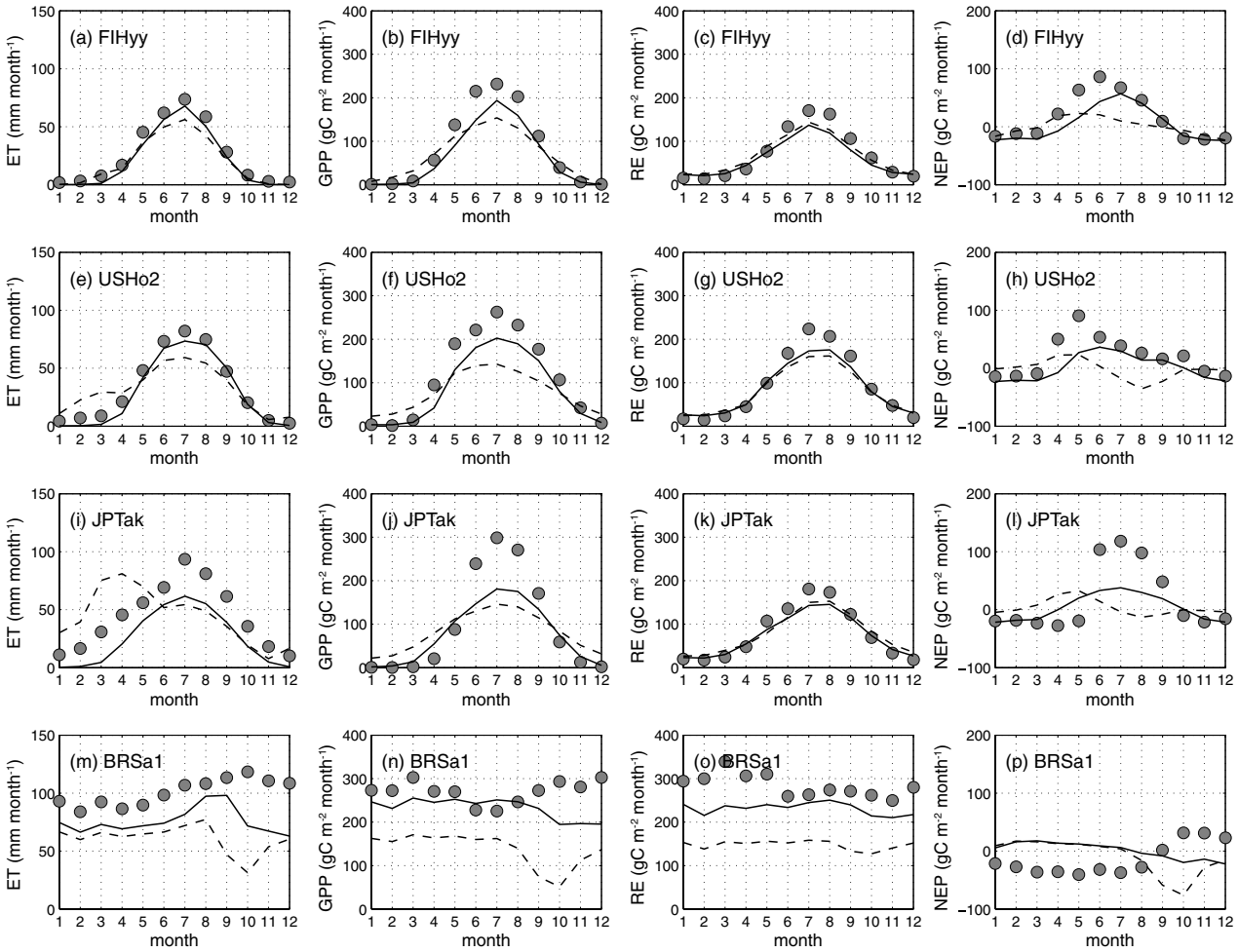

Fig. 3. Observed (dotted) and simulated [default (dotted line) and improved terrestrial submodel (solid line)] monthly variations in ET, GPP, RE and NEP at four eddy covariance observation sites, (a–d) Hyyti (FIHyy) (e–h) Howland (USHow), (i–l) Takayama (JPTak) and (m–p) Tapajos (BRSa1) in the off-line experiment. Monthly variations were calculated by averaging over the observation period.

parameters (shown below) were selected and tuned to fit the observed seasonal water and carbon cycles. Third, changes in model structure were limited to the snow submodel only. Since the snow submodel itself is independent from other components with few degrees of freedom in the structure, objectivities of the submodel modification are mostly retained. These model modifications were conducted by hand, and the best parameters were determined through comparison with seasonal variations of the water and carbon budget. As a result, to improve them, we applied the following four modifications: (1) the snow sublimation and melting model was modified to prevent anomalous large sublimation during the snow season, (2) the quantum efficiency of photosynthesis and the nitrogen concentration were increased to enhance magnitude of GPP, (3) the temperature sensitivity of photosynthesis was changed to remove biases of GPP overestimation during spring and autumn and (4) deeper rooting depth (1.5 m) was set to prevent sudden GPP decline by water stress during the dry season in the tropics. Details of the model parameters are given in Table 2. Most of these modifications have been previously reported in other terrestrial ecosystem modelling studies. For example, Ichii et al. (2008) reported that the underestimation of snow cover in the Biome-BGC terrestrial ecosystem model (Thornton et al., 2002) causes biases of seasonal water and carbon cycle. Zaehle et al. (2005) reported that the photosynthesis efficiency parameter is one of the most sensitive parameters to determine the magnitude of photosynthesis in the Lund-Potsdam-Jena Dynamic Global Vegetation Model (LPJ-DGVM). Ichii et al. (2007, 2009) reported that setting of rooting depth in the terrestrial ecosystem model significantly affects seasonal patterns in modelled ET and GPP in a seasonally dry environment.

By applying these modifications, the terrestrial submodel was greatly improved (Fig. 2) compared with the results from the default model simulations. For example, the slopes of the regression lines became closer to 1, changing from 0.52 to 0.76 for ET, 0.36 to 0.64 for GPP, 0.48 to 0.71 for RE, and 0.02 to

Table 2. Model parameter used in this study

Parameter		Description	Default value	Modified value
d_r		Rooting depth (m)	1.0	1.5
α	(C_3 plants)	Quantum efficiency (mol CO_2/mol PAR photons)	0.06	0.08
n_l	(BT)	Top leaf nitrogen concentration (kg N/kg C)	0.036	0.040
T_{low}	(BT)	Lower temperature for photosynthesis (°C)	−5.0	12.0
	(NT)		−10.0	8.0
	(C_3G)		−5.0	10.0
	(C_4G)		8.0	10.0
	(S)		−5.0	10.0
T_{upp}	(BT)	Upper temperature for photosynthesis (°C)	33.0	36.0
	(NT)		28.0	31.0
	(C_3G)		33.0	36.0
	(C_4G)		42.0	45.0
	(S)		33.0	36.0

Note: Abbreviations for PFT: broadleaf tree (BT), needleleaf tree (NT), C_3 grass (C_3G), C_4 grass (C_4G) and shrub (S).

0.26 for NEP. The correlation became better than those from the default model simulations ($R^2 = 0.57$ to 0.69, 0.64 to 0.68, 0.69 to 0.69 and 0.00 to 0.26 for ET, GPP, RE and NEP, respectively).

Refinement of the terrestrial submodel also improved the simulation of the seasonal variation of water and carbon fluxes (Fig. 3). For ET, overestimation during the snow season and underestimation of seasonal amplitude were greatly improved (Figs 3a, e, i and m). In USHo2 and JPTak, the anomalous ET overestimations during the snow cover season were removed by the model refinement (Figs 3e and i). In FIHyy and USHo2, seasonal variations of ET were more accurately simulated (Figs 3a and e). For GPP and RE, underestimation of the seasonal peak was also greatly improved at most sites (Figs 3b, c, f, g, j, k, n and o). In FIHyy and USHo2, simulated seasonal variation of GPP and RE were closer to observed data overall (Figs 3b, c, f and g). In JPTak, underestimation of peak GPP in summer and overestimation of GPP in spring and autumn were improved (Fig. 3j). In BRSa1, magnitude of GPP and RE became closer to the observed magnitudes. For these seasonal variations, the biases of rapid decline during the dry season were removed (Figs 3n and o). For NEP, the seasonal variation (e.g. seasonal amplitude and phase) slightly improved (Figs 3d, h, l and p), probably due to lack of a site history effect in the model. In all sites, simulated NEP comparatively improved; however, there is still room for improvement.

After the refinement, the model successfully reduced the RMSE of observed and simulated monthly variation in ET, GPP, RE and NEP at most sites (Fig. 4). The number of sites where RMSE was reduced after the model improvement was 28, 33, 17 and 35 sites for ET, GPP, RE and NEP, respectively. For seasonal variation of ET, GPP and NEP, we found improvement at more sites (more than half of the total); however, only about one-third of the all sites were improved for RE. The poor improvement of RE is probably caused by the effect of land use and management change, which we did not include in this analysis.

4.2. ESM experiments

4.2.1. Point scale analysis. The refinement of the terrestrial submodel also improves ESM simulation at a point scale (Fig. 5). The ESM with the default terrestrial submodel mostly underestimates the monthly ET and carbon fluxes at all sites. Once we replaced the default terrestrial submodel with the improved one in the ESM, the simulation results of ET and carbon fluxes were greatly improved. The slopes of the regression line were increased toward 1 (0.58 to 0.94 for ET, 0.36 to 0.70 for GPP, 0.49 to 0.77 for RE and 0.05 to 0.26 for NEP), and higher correlation resulted ($R^2 = 0.50$ to 0.70, 0.47 to 0.61, 0.60 to 0.61 and 0.01 to 0.22 for ET, GPP, RE and NEP, respectively). There is a room for further improvements especially for the NEP. Potential causes are biases of the atmosphere submodel and differences in the spatial scales of a grid in the ESM and a footprint of observations.

4.2.2. Global scale carbon cycle and climate analysis. Improvement of the terrestrial submodel also has effects on the simulated time variations of global climate and carbon cycle based on the ESM. Simulated atmospheric CO_2 concentration by the improved ESM (UVic-ESCM with the improved terrestrial submodel) was 100 ppmv lower in 2100 than that determined with the default ESM (UVic-ESCM with the default terrestrial submodel) (Fig. 6a). Change of the carbon budget also influenced simulated climate. Simulated global averaged temperature indicated a gradual rise compared with the default model and the difference is about 0.7 K in 2100 (Fig. 6b). As a result, the increase of the global averaged temperature is estimated to be about 3 K relative to 1850 by 2100.

One of the potential causes of difference in atmospheric CO_2 and global temperature is increased land carbon uptake in the

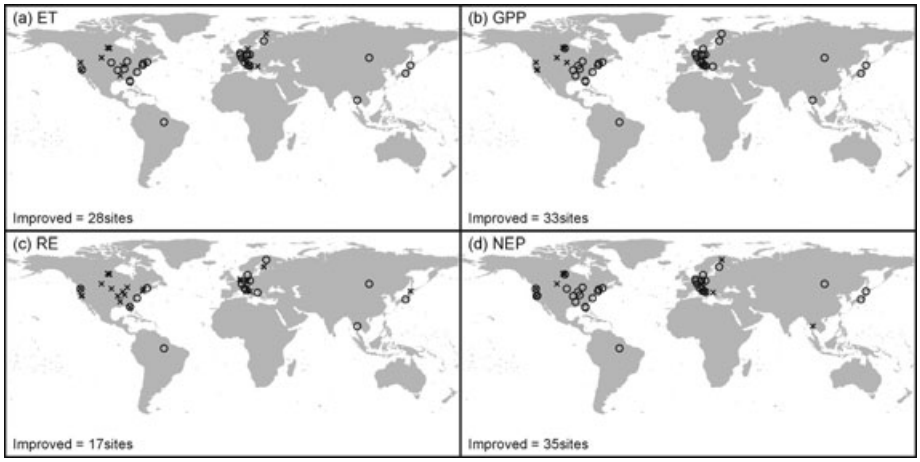

Fig. 4. Effect of the model improvements on RMSE between observed and simulated (a) ET, (b) GPP, (c) RE and (d) NEP at a monthly scale for the off-line experiment. The sites with decreasing and increasing RMSE by the terrestrial submodel improvements are marked by O and X, respectively.

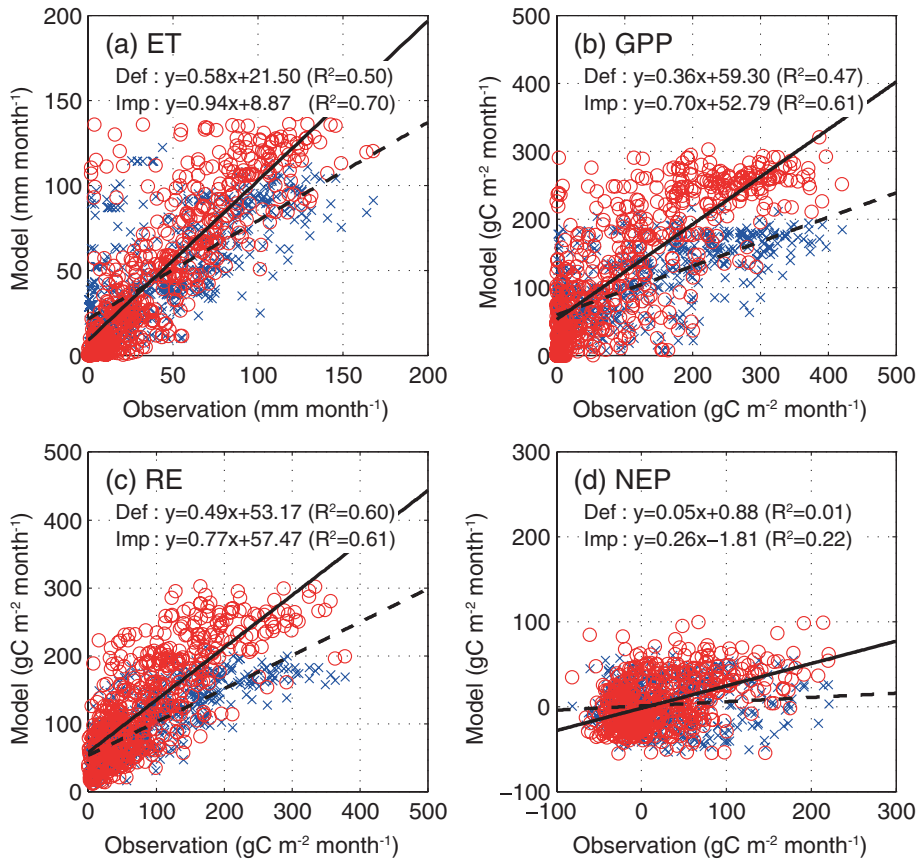

Fig. 5. Observed and modelled (default (blue) and improved (red) terrestrial submodel in the ESM experiment) monthly variations in (a) ET, (b) GPP, (c) RE and (d) NEP for all sites.

simulation by the ESM with the improved terrestrial submodel. The result of the improved ESM showed a more upward trend of GPP and RE with a larger gradient than that observed with the default ESM (Figs 6c and d), which results in dramatic changes in NEP. Although the default ESM simulated a rapid NEP decrease after 2050, the improved one showed an increase (Fig. 6e). The changes resulted in a change in the terrestrial carbon reservoir (i.e. vegetation and soil). Simulated change in vegetation carbon showed that an increment in vegetation carbon was much the same in both the default and improved

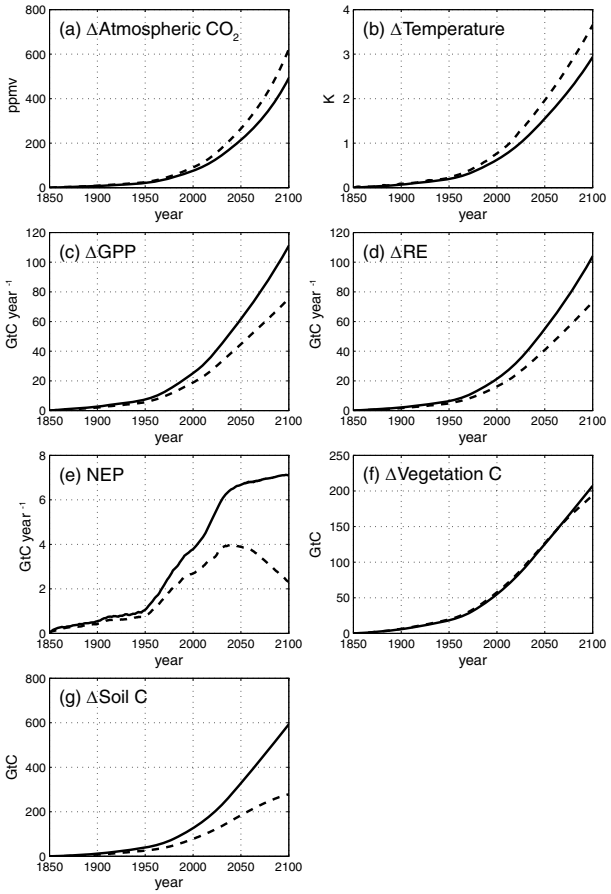

Fig. 6. Default submodel (dotted line)—and refined submodel (solid line)—ESM simulated (a) atmospheric CO_2 concentration, (b) annual average temperature, (c) total GPP, (d) total RE, (e) total NEP, (f) total vegetation carbon and (g) total soil carbon at a global scale. Differences from initial status (year 1850) are shown except for (e).

model simulations (Fig. 6f). In contrast, a simulated change in soil carbon indicated a great increase by 2100 using the improved model (Fig. 6g). The value was twice as high as compared with estimated soil carbon by the default model. Thus, increasing soil carbon is thought to contribute to an increase in NEP.

5. Discussion

This study could provide an important contribution to the ESM community toward the reduction of the uncertainties among models. One of the causes of the uncertainties in ESM comes from uncertainty in terrestrial submodels. This study demonstrated that (1) a terrestrial submodel included in an ESM needs refinements made by use of observation and (2) the submodel refinement has an impact on carbon cycle and climate simulation at both the point and global scales in the ESM. The potential contribution to the ESM community and remaining problems are described in this section.

Evaluation of the terrestrial submodel is a very important initial step to evaluate ESMs. First, we found biases of underestimation in terrestrial carbon cycle seasonality at multiple point scales. These biases potentially affect the online simulation and future projection of the carbon cycle and climate. Through confirmation of these biases and their causes, we found and fixed several potential problems in terrestrial submodels. However, most current ESMs are not evaluated well at the regional and global scales. These insufficient validations can cause large uncertainties in future projection.

Second, isolating the terrestrial submodel from an ESM is also effective for analysing the causes of the uncertainties inside ESMs. In this analysis, by extracting the terrestrial submodel, we found an effective framework for testing and refining the ESM. We conducted an assessment of the terrestrial submodel and replaced it with the improved one within the ESM. We found that the difference between the coupled model before and after terrestrial submodel refinements is mainly caused by the terrestrial submodel refinement. The remaining differences may be caused by the errors in climate data and/or the coupled effect of carbon cycle and climate.

Third, establishment of a systematic procedure that is applicable to other models is an effective way to improve ESMs. We tested the procedure to first evaluate the terrestrial submodel in an off-line mode and then evaluated an ESM in the coupled mode. The procedure itself is applicable to other ESMs, and useful for benchmarking and running ESMs. Furthermore, this work can be strengthened by including more systematic and objective model evaluation and refinement (Stockli et al., 2008; Randerson et al., 2009; Wang et al., 2009) using more eddy covariance observation sites and satellite-based products. More objective and systematic terrestrial model improvements will successfully improve the ecosystem models and ESMs.

Although this study proposed an effective case study for ESMs, and tested it within an ESM framework, there still remain several potential problems. First, the difference of spatial scales between ESMs and point observations of eddy covariance should be solved in the future. The footprint of eddy covariance observation (several km) is greatly different from that of ESM (in this study, $1.8^\circ \times 3.6^\circ$). These differences can potentially affect the climate forcing to the terrestrial model. Different land cover types might be captured by the ESM due to insufficient atmospheric and terrestrial submodels. Therefore, further improvements of them are required. Moreover, geographical distribution of eddy covariance observation sites was biased to the northern hemisphere. Currently, several studies have described spatial upscaling techniques using eddy covariance observations, gridded climate data and satellite-based data (Papale and Valentini, 2003; Yang et al., 2007; Xiao et al., 2008; Jung et al., 2009). Use of these data as validation data for terrestrial ecosystem models can potentially improve the modelling.

Second, carbon cycle modelling in tropical forests is still uncertain, and needs further assessment to represent observed

seasonality. Several studies pointed out the importance of deep rooting depth (e.g. Ichii et al., 2007; Baker et al., 2008), leaf phonological states (e.g. Baker et al., 2008; Poulter et al., 2009), hydraulic redistribution (Lee et al., 2005; Baker et al., 2008), and moisture control on soil respiration (e.g. Hutyra et al., 2007; Baker et al., 2008). Study of these mechanisms is still at a very early stage, which prevents their incorporation into the terrestrial submodels in ESMs. To evaluate the effects on the tropical forest vulnerability, such as forest dieback (e.g. Cox et al., 2000), we need to incorporate these mechanisms into the model.

Third, human effects on terrestrial ecosystems, such as disturbance and fire, were not included in the study. Several studies identified the effect of site history on the terrestrial carbon budget. These effects have already been included in the eddy covariance observations (Thornton et al., 2002; Law et al., 2003; Magnani et al., 2007). Lack of site history can also be a potential cause of poor correlation between observed and modelled RE and NEP. Therefore, future studies need to include site history.

Fourth, the atmosphere submodel also needs improvements. We demonstrated that the differences between off-line and online simulations are still large, although the model is improved in both off-line and online simulations. One of the potential causes of the differences is that the climate model is simply described by a two-dimensional energy balance model. However, several studies have found that the responses of climate model to simulate future changes are also different and climate model-dependent (Berthelot et al., 2005; Ito, 2005). Similar to this study, the atmosphere model should be also evaluated independently and coupled to ESMs.

Finally, more objective methods of model parameter calibration such as to apply optimization routine (Williams et al., 2009) and hierarchical analysis (Wang et al., 2009) are needed. In this study, we tuned parameter in an iterative way, and still biases were remained in the terrestrial submodels. These biases are partly due to insufficient model parameter tuning. Use of these sophisticated methods potentially helps to reduce the difference between model outputs and observations.

6. Conclusion

In this study, we evaluated and improved a terrestrial ecosystem submodel (MOSES2/TRIFFID) included in an ESM (UVic-ESCM) using eddy covariance observations. Then, we tested the effects of terrestrial submodel improvements on future projection of global carbon cycle and climate based on ESM. We found that the default terrestrial submodel in the ESM is immature. Through fixing parameters and models structures, the submodel was greatly improved by using eddy covariance observations as constraints. The terrestrial submodel improvement also affected the simulation of carbon cycle and climate coupled model both at point and global scales. Therefore, to improve ESM and reduce their uncertainties, terrestrial submodels should be evaluated and refined.

7. Acknowledgments

This study was financially supported by the A3 Foresight Program (CarboEastAsia: Capacity building among ChinaFlux, JapanFlux, and KoFlux to cope with climate change protocols by synthesizing measurement, theory, and modeling in quantifying and understanding of carbon fluxes and storages in East Asia) by JSPS, the National Natural Science Foundation of China (NSFC), and the Korea Science and Engineering Foundation (KOSEF) and Grant-in-Aid for Scientific Research (C) (ID: 50345865) from the Japan Society for the Promotion of Science (JSPS). The data were provided by the CarboEastAsia database. Special thanks to all scientists and supporting teams at the AmeriFlux, CarboEurope and AsiaFlux sites. We also acknowledge two anonymous reviewers for their valuable comments on this manuscript.

Reference

Abramowitz, G., Leuning, R., Clark, M. and Pitman, A. 2008. Evaluating the performance of land surface models. *J. Clim.* **21**, 5468–5481.

Anthoni, P. M., Knohl, A., Rebmann, C., Freibauer, A., Mund, M. and co-authors. 2004. Forest and agricultural land-use-dependent CO_2 exchange in Thuringia, Germany. *Global Change Biol.* **10**, 2005–2019.

Aubinet, M., Chermanne, B., Vandenhaute, M., Longdoz, B., Yernaux, M. and co-authors. 2001. Long term carbon dioxide exchange above a mixed forest in the Belgian Ardennes. *Agric. Forest Meteorol.* **108**, 293–315.

Baker, I. T., Prihodko, L., Denning, A. S., Goulden, M., Miller, S. and co-authors. 2008. Seasonal drought stress in the Amazon: reconciling models and observations. *J. Geophys. Res.-Biogeosci.* **113**, G00B01, doi:10.1029/2007JG000644.

Bala, G., Caldeira, K., Mirin, A., Wickett, M., Delire, C. and co-authors. 2006. Biogeophysical effects of CO_2 fertilization on global climate. *Tellus* **58B**, 620–627.

Baldocchi, D. 2008. 'Breathing' of the terrestrial biosphere: lesson learned from a global network of carbon dioxide flux mesurement systems. Turner Review No. 15, *Aust. J. Bot.* **56**, 1–26.

Baldocchi, D., Falge, E., Gu, L. H., Olson, R., Hollinger, D. and co-authors. 2001. FLUXNET: a new tool to study the temporal and spatial variability of ecosystem-scale carbon dioxide, water vapor, and energy flux densities. *Bull. Am. Meteorol. Soc.* **82**, 2415–2434.

Baldocchi, D. D., Xu, L. K. and Kiang, N. 2004. How plant functional-type, weather, seasonal drought, and soil physical properties alter water and energy fluxes of an oak-grass savanna and an annual grassland. *Agric. Forest Meteorol.* **123**, 13–39.

Berthelot, M., Friedlingstein, P., Ciais, P., Dufresne, J. L. and Monfray, P. 2005. How uncertainties in future climate change predictions translate into future terrestrial carbon fluxes. *Global Change Biol.* **11**, 959–970.

Bitz, C. M., Holland, M. M., Weaver, A. J. and Eby, M. 2001. Simulating the ice-thickness distribution in a coupled climate model. *J. Geophys. Res.-Oceans* **106**, 2441–2463.

Collatz, G. J., Ball, J. T., Grivet, C. and Berry, J. A. 1991. Physiological and environmental-regulaton of stomatal conductance, photosynthesis and transpiration—a model that includes a laminar boundary-layer. *Agric. Forest Meteorol.* **54**, 107–136.

Collatz, G. J., Ribas-Carbo, M. and Berry, J. A. 1992. Coupled photosynthesis-stomatal conductance model for leaves of C4 plants. *Aust. J. Plant Physiol.* **19**, 519–538.

Cox, P. M. 2001. Description of the "TRIFFID" Dynamic Global Vegetation Model. Hadley Center Technical Note 24. Met Office, UK.

Cox, P. M., Betts, R. A., Bunton, C. B., Essery, R. L. H., Rowntree, P. R. and co-authors. 1999. The impact of new land surface physics on the GCM simulation of climate and climate sensitivity. *Clim. Dyn.* **15**, 183–203.

Cox, P. M., Betts, R. A., Jones, C. D., Spall, S. A. and Totterdell, I. J. 2000. Acceleration of global warming due to carbon-cycle feedbacks in a coupled climate model. *Nature* **408**, 184–187.

Dufresne, J. L., Friedlingstein, P., Berthelot, M., Bopp, L., Ciais, P. and co-authors. 2002. On the magnitude of positive feedback between future climate change and the carbon cycle. *Geophys. Res. Lett.* **29**, 1405, doi:10.1029/2001GL013777.

Essery, R. and Clark, D. B. 2003. Developments in the MOSES 2 land-surface model for PILPS 2e. *Global Planet. Change* **38**, 161–164.

Etheridge, D. M., Steele, L. P., Langenfelds, R. L., Francey, R. J., Barnola, J. M. and co-authors. 1998. Historical CO_2 records from the Law Dome DE08, DE08–2, and DSS ice cores. In: *Trends: A Compendium of Data on Global Change*. Carbon Dioxide Information Analysis Center, Oak Ridge National Laboratory, U.S. Department of Energy, Oak Ridge, Tenn., USA.

Friedlingstein, P., Cox, P., Betts, R., Bopp, L., Von Bloh, W. and co-authors. 2006. Climate-carbon cycle feedback analysis: results from the (CMIP)-M-4 model intercomparison. *J. Clim.* **19**, 3337–3353.

Gilmanov, T. G., Tieszen, L. L., Wylie, B. K., Flanagan, L. B., Frank, A. B. and co-authors. 2005. Integration of CO_2 flux and remotely-sensed data for primary production and ecosystem respiration analyses in the Northern Great Plains: potential for quantitative spatial extrapolation. *Global Ecol. Biogeogr.* **14**, 271–292.

Goldstein, A. H., Hultman, N. E., Fracheboud, J. M., Bauer, M. R., Panek, J. A. and co-authors. 2000. Effects of climate variability on the carbon dioxide, water, and sensible heat fluxes above a ponderosa pine plantation in the Sierra Nevada (CA). *Agric. Forest Meteorol.* **101**, 113–129.

Gough, C. M., Vogel, C. S., Schmid, H. P., Su, H. B. and Curtis, P. S. 2008. Multi-year convergence of biometric and meteorological estimates of forest carbon storage. *Agric. Forest Meteorol.* **148**, 158–170.

Goulden, M. L., Miller, S. D., da Rocha, H. R., Menton, M. C., de Freitas, H. C. and co-authors. 2004. Diel and seasonal patterns of tropical forest CO_2 exchange. *Ecol. Appl.* **14**, S42-S54.

Granier, A., Ceschia, E., Damesin, C., Dufrene, E., Epron, D. and co-authors. 2000. The carbon balance of a young Beech forest. *Funct. Ecol.* **14**, 312–325.

Gu, L. H., Meyers, T., Pallardy, S. G., Hanson, P. J., Yang, B. and co-authors. 2006. Direct and indirect effects of atmospheric conditions and soil moisture on surface energy partitioning revealed by a prolonged drought at a temperate forest site. *J. Geophys. Res.-Atmos.* **111**, D16102, doi:10.1029/2006JD007161.

Gu, L. H., Meyers, T., Pallardy, S. G., Hanson, P. J., Yang, B. and co-authors. 2007. Influences of biomass heat and biochemical energy storages on the land surface fluxes and radiative temperature. *J. Geophys. Res.-Atmos.* **112**, D02107, doi:10.1029/2006JD007425.

Hirata, R., Hirano, T., Saigusa, N., Fujinuma, Y., Inukai, K. and co-authors. 2007. Seasonal and interannual variations in carbon dioxide exchange of a temperate larch forest. *Agric. Forest Meteorol.* **147**, 110–124.

Hirata, R., Saigusa, N., Yamamoto, S., Ohtani, Y., Ide, R. and co-authors. 2008. Spatial distribution of carbon balance in forest ecosystems across East Asia. *Agric. Forest Meteorol.* **148**, 761–775.

Hollinger, D. Y., Goltz, S. M., Davidson, E. A., Lee, J. T., Tu, K. and co-authors. 1999. Seasonal patterns and environmental control of carbon dioxide and water vapour exchange in an ecotonal boreal forest. *Global Change Biol.* **5**, 891–902.

Hollinger, D. Y., Aber, J., Dail, B., Davidson, E. A., Goltz, S. M. and co-authors. 2004. Spatial and temporal variability in forest-atmosphere CO_2 exchange. *Global Change Biol.* **10**, 1689–1706.

Hutyra, L. R., Munger, J. W., Saleska, S. R., Gottlieb, E., Daube, B. C. and co-authors. 2007. Seasonal controls on the exchange of carbon and water in an Amazonian rain forest. *J. Geophys. Res.-Biogeosci.* **112**, G03008, doi:10.1029/2006JG000365.

Ichii, K., Matsui, Y., Murakami, K., Mukai, T., Yamaguchi, Y. and co-authors. 2003. A simple global carbon and energy coupled cycle model for global warming simulation: sensitivity to the light saturation effect. *Tellus* **55B**, 676–691.

Ichii, K., Hashimoto, H., White, M. A., Potters, C., Hutyra, L. R. and co-authors. 2007. Constraining rooting depths in tropical rainforests using satellite data and ecosystem modeling for accurate simulation of gross primary production seasonality. *Global Change Biol.* **13**, 67–77.

Ichii, K., White, M. A., Votava, P., Michaelis, A. and Nemani, R. R. 2008. Evaluation of snow models in terrestrial biosphere models using ground observation and satellite data: impact on terrestrial ecosystem processes. *Hydrol. Process.* **22**, 347–355.

Ichii, K., Wang, W. L., Hashimoto, H., Yang, F. H., Votava, P. and co-authors. 2009. Refinement of rooting depths using satellite-based evapotranspiration seasonality for ecosystem modeling in California. *Agric. Forest Meteorol.* **149**, 1907–1918.

Irvine, J., Law, B. E. and Hibbard, K. A. 2007. Postfire carbon pools and fluxes in semiarid ponderosa pine in Central Oregon. *Global Change Biol.* **13**, 1748–1760.

Ito, A. 2005. Climate-related uncertainties in projections of the twenty-first century terrestrial carbon budget: off-line model experiments using IPCC greenhouse-gas scenarios and AOGCM climate projections. *Climate Dyn.* **24**, 435–448.

Jenkins, J. P., Richardson, A. D., Braswell, B. H., Ollinger, S. V., Hollinger, D. Y. and co-authors. 2007. Refining light-use efficiency calculations for a deciduous forest canopy using simultaneous tower-based carbon flux and radiometric measurements. *Agric. Forest Meteorol.* **143**, 64–79.

Jones, C. D., Cox, P. and Huntingford, C. 2003. Uncertainty in climate-carbon-cycle projections associated with the sensitivity of soil respiration to temperature. *Tellus* **55B**, 642–648.

Joos, F., Prentice, I. C., Sitch, S., Meyer, R., Hooss, G. and co-authors. 2001. Global warming feedbacks on terrestrial carbon uptake under the Intergovernmental Panel on Climate Change (IPCC) emission scenarios. *Global Biogeochem. Cycles* **15**, 891–907.

Jung, M., Reichstein, M. and Bondeau, A. 2009. Towards global empirical upscaling of FLUXNET eddy covariance observations: validation of a model tree ensemble approach using a biosphere model. *Biogeosciences* **6**, 2001–2013.

Kalnay, E., Kanamitsu, M., Kistler, R., Collins, W., Deaven, D. and co-authors. 1996. The NCEP/NCAR 40-year reanalysis project. *Bull. Am. Meteorol. Soc.* **77**, 437–471.

Kato, T., Ito, A. and Kawamiya, M. 2009. Multiple temporal scale variability during the twentieth century in global carbon dynamics simulated by a coupled climate-terrestrial carbon cycle model. *Clim. Dyn.* **32**, 901–923.

Keeling, R. F., Piper, S. C., Bollenbacher, A. F. and Walker, J. S. 2009. Atmospheric CO_2 records from sites in the SIO air sampling network. In: *Trends: A Compendium of Data on Global Change*. Carbon Dioxide Information Analysis Center, Oak Ridge National Laboratory, U.S. Department of Energy, Oak Ridge, Tenn., USA, doi:10.3334/CDIAC/atg.035.

Kheshgi, H. S. and Jain, A. K. 2003. Projecting future climate change: implications of carbon cycle model intercomparisons. *Global Biogeochem. Cycles* **17**, 1047, doi:10.1029/2001GB001842.

Knohl, A., Schulze, E. D., Kolle, O. and Buchmann, N. 2003. Large carbon uptake by an unmanaged 250-year-old deciduous forest in Central Germany. *Agric. Forest Meteorol.* **118**, 151–167.

Kowalski, A. S., Loustau, D., Berbigier, P., Manca, G., Tedeschi, V. and co-authors. 2004. Paired comparisons of carbon exchange between undisturbed and regenerating stands in four managed forests in Europe. *Global Change Biol.* **10**, 1707–1723.

Kucharik, C. J., Barford, C. C., El Maayar, M., Wofsy, S. C., Monson, R. K. and co-authors. 2006. A multiyear evaluation of a Dynamic Global Vegetation Model at three AmeriFlux forest sites: vegetation structure, phenology, soil temperature, and CO_2 and H_2O vapor exchange. *Ecol. Modell.* **196**, 1–31.

Law, B. E., Sun, O. J., Campbell, J., Van Tuyl, S. and Thornton, P. E. 2003. Changes in carbon storage and fluxes in a chronosequence of ponderosa pine. *Global Change Biol.* **9**, 510–524.

Law, B. E., Turner, D., Campbell, J., Sun, O. J., Van Tuyl, S. and co-authors. 2004. Disturbance and climate effects on carbon stocks and fluxes across Western Oregon USA. *Global Change Biol.* **10**, 1429–1444.

Lee, J. E., Oliveira, R. S., Dawson, T. E. and Fung, I. 2005. Root functioning modifies seasonal climate. *Proc. Natl. Acad. Sci. U. S. A.* **102**, 17576–17581.

Lenton, T. M. 2000. Land and ocean carbon cycle feedback effects on global warming in a simple Earth system model. *Tellus* **52B**, 1159–1188.

Li, S. G., Asanuma, J., Kotani, A., Eugster, W., Davaa, G. and co-authors. 2005. Year-round measurements of net ecosystem CO_2 flux over a montane larch forest in Mongolia. *J. Geophys. Res.-Atmos.* **110**, D09303, doi:10.1029/2004JD005453.

Ma, S. Y., Baldocchi, D. D., Xu, L. K. and Hehn, T. 2007. Inter-annual variability in carbon dioxide exchange of an oak/grass savanna and open grassland in California. *Agric. Forest Meteorol.* **147**, 157–171.

Magnani, F., Mencuccini, M., Borghetti, M., Berbigier, P., Berninger, F. and co-authors. 2007. The human footprint in the carbon cycle of temperate and boreal forests. *Nature* **447**, 848–850.

Mahecha, M. D., Reichstein, M., Jung, M., Seneviratne, S. I., Zaehle, S. and co-authors. 2010. Comparing observations and process-based simulations of biosphere-atmosphere exchanges on multiple time scales. *J. Geophys. Res.-Biogeosci.*, **115**, G02003, doi:10.1029/2009JG001016.

Marland, G., Boden, T. A., Andres, R. J. 2005. Global, regional, and national CO_2 emissions. In: *Trends: A Compendium of Data on Global Change*. Carbon Dioxide Information Analysis Center, Oak Ridge National Laboratory, U.S. Department of Energy, Oak Ridge, TN, USA.

Matthews, H. D., Eby, M., Weaver, A. J. and Hawkins, B. J. 2005a. Primary productivity control of simulated carbon cycle-climate feedbacks. *Geophys. Res. Lett.* **32**, L14708, doi:10.1029/2005GL022941.

Matthews, H. D., Weaver, A. J. and Meissner, K. J. 2005b. Terrestrial carbon cycle dynamics under recent and future climate change. *J. Clim.* **18**, 1609–1628.

Matthews, H. D. and Caldeira, K. 2008. Stabilizing climate requires near-zero emissions. *Geophys. Res. Lett.* **35**, L04705, doi:10.1029/2007GL032388.

Matthews, H. D., Gillett, N. P., Stott, P. A. and Zickfeld, K. 2009. The proportionality of global warming to cumulative carbon emissions. *Nature* **459**, 829–823.

McMillan, A. M. S., Winston, G. C. and Goulden, M. L. 2008. Age-dependent response of boreal forest to temperature and rainfall variability. *Global Change Biol.* **14**, 1904–1916.

Medlyn, B. E., Robinson, A. P., Clement, R. and McMurtrie, R. E. 2005. On the validation of models of forest CO_2 exchange using eddy covariance data: some perils and pitfalls. *Tree Physiol.* **25**, 839–857.

Meissner, K. J., Weaver, A. J., Matthews, H. D. and Cox, P. M. 2003. The role of land surface dynamics in glacial inception: a study with the UVic Earth System Model. *Clim. Dyn.* **21**, 515–537.

Misson, L., Tu, K. P., Boniello, R. A. and Goldstein, A. H. 2006. Seasonality of photosynthetic parameters in a multi-specific and vertically complex forest ecosystem in the Sierra Nevada of California. *Tree Physiol.* **26**, 729–741.

Miyama, T. and Kawamiya, M. 2009. Estimating allowable carbon emission for CO_2 concentration stabilization using a GCM-based Earth system model. *Geophys. Res. Lett.* **36**, L19709, doi:10.1029/2009GL039678.

Moffat, A. M., Papale, D., Reichstein, M., Hollinger, D. Y., Richardson, A. D. and co-authors. 2007. Comprehensive comparison of gap-filling techniques for eddy covariance net carbon fluxes. *Agric. Forest Meteorol.* **147**, 209–232.

Morales, P., Sykes, M. T., Prentice, I. C., Smith, P., Smith, B. and co-authors. 2005. Comparing and evaluating process-based ecosystem model predictions of carbon and water fluxes in major European forest biomes. *Global Change Biol.* **11**, 2211–2233.

O'Ishi, R. and Abe-Ouchi, A. 2009. Influence of dynamic vegetation on climate change arising from increasing CO_2. *Clim. Dyn.* **33**, 645–663.

O'Ishi, R., Abe-Ouchi, A., Prentice, I. C. and Sitch, S. 2009. Vegetation dynamics and plant CO_2 responses as positive feedbacks in a greenhouse world. *Geophys. Res. Lett.* **36**, L11706, doi:10.1029/2009GL038217.

Oren, R., Ewers, B. E., Todd, P., Phillips, N. and Katul, G. 1998. Water balance delineates the soil layer in which moisture affects canopy conductance. *Ecol. Appl.* **8**, 990–1002.

Oren, R., Hseih, C. I., Stoy, P., Albertson, J., McCarthy, H. R. and co-authors. 2006. Estimating the uncertainty in annual net ecosystem carbon exchange: spatial variation in turbulent fluxes and sampling errors in eddy-covariance measurements. *Global Change Biol.* **12**, 883–896.

Pacanowski, R. 1995. MOM2 Documentation User's Guide and Reference Manual. GFDL Ocean Group Technical Report, NOAA, GFDL, Princeton, USA, 232.

Papale, D. and Valentini, A. 2003. A new assessment of European forests carbon exchanges by eddy fluxes and artificial neural network spatialization. *Global Change Biol.* **9**, 525–535.

Pilegaard, K., Hummelshoj, P., Jensen, N. O. and Chen, Z. 2001. Two years of continuous CO_2 eddy-flux measurements over a Danish beech forest. *Agric. Forest Meteorol.* **107**, 29–41.

Poulter, B., Heyder, U. and Cramer, W. 2009. Modeling the sensitivity of the seasonal cycle of GPP to dynamic LAI and soil depths in tropical rainforests. *Ecosystems* **12**, 517–533.

Powell, T. L., Gholz, H. L., Clark, K. L., Starr, G., Cropper, W. P. and co-authors. 2008. Carbon exchange of a mature, naturally regenerated pine forest in north Florida. *Global Change Biol.* **14**, 2523–2538.

Randerson, J. T., Hoffman, F. M., Thornton, P. E., Mahowald, N. M., Lindsay, K. and co-authors. 2009. Systematic assessment of terrestrial biogeochemistry in coupled climate-carbon models. *Global Change Biol.* **15**, 2462–2484.

Rannik, U., Keronen, P., Hari, P. and Vesala, T. 2004. Estimation of forest-atmosphere CO_2 exchange by eddy covariance and profile techniques. *Agric. Forest Meteorol.* **126**, 141–155.

Reichstein, M., Falge, E., Baldocchi, D., Papale, D., Aubinet, M. and co-authors. 2005. On the separation of net ecosystem exchange into assimilation and ecosystem respiration: review and improved algorithm. *Global Change Biol.* **11**, 1424–1439.

Saigusa, N., Yamamoto, S., Murayama, S., Kondo, H. and Nishimura, N. 2002. Gross primary production and net ecosystem exchange of a cool-temperate deciduous forest estimated by the eddy covariance method. *Agric. Forest Meteorol.* **112**, 203–215.

Saigusa, N., Yamamoto, S., Hirata, R., Ohtani, Y., Ide, R. and co-authors. 2008. Temporal and spatial variations in the seasonal patterns of CO_2 flux in boreal, temperate, and tropical forests in East Asia. *Agric. Forest Meteorol.* **148**, 700–713.

Saleska, S. R., Miller, S. D., Matross, D. M., Goulden, M. L., Wofsy, S. C. and co-authors. 2003. Carbon in amazon forests: unexpected seasonal fluxes and disturbance-induced losses. *Science* **302**, 1554–1557.

Schmid, H. P., Grimmond, C. S. B., Cropley, F., Offerle, B. and Su, H. B. 2000. Measurements of CO_2 and energy fluxes over a mixed hardwood forest in the mid-western United States. *Agric. Forest Meteorol.* **103**, 357–374.

Siqueira, M. B., Katul, G. G., Sampson, D. A., Stoy, P. C., Juang, J.-Y. and co-authors. 2006. Multiscale model intercomparisons of CO_2 and H_2O exchange rates in a maturing southeastern US pine forest. *Global Change Biol.* **12**, 1189–1207.

Stockli, R., Lawrence, D. M., Niu, G. Y., Oleson, K. W., Thornton, P. E. and co-authors. 2008. Use of FLUXNET in the community land model development. *J. Geophys. Res.-Biogeosci.* **113**, G01025, doi:10.1029/2007JG000562.

Tanja, S., Berninger, F., Vesala, T., Markkanen, T., Hari, P. and co-authors. 2003. Air temperature triggers the recovery of evergreen boreal forest photosynthesis in spring. *Global Change Biol.* **9**, 1410–1426.

Thompson, S. L., Govindasamy, B., Mirin, A., Caldeira, K., Delire, C. and co-authors. 2004. Quantifying the effects of CO_2-fertilized vegetation on future global climate and carbon dynamics. *Geophys. Res. Lett.* **31**, L23211, doi:10.1029/2004GL021239.

Thornton, P. E., Law, B. E., Gholz, H. L., Clark, K. L., Falge, E. and co-authors. 2002. Modeling and measuring the effects of disturbance history and climate on carbon and water budgets in evergreen needleleaf forests. *Agric. Forest Meteorol.* **113**, 185–222.

Van Dijk, A. and Dolman, A. J. 2004. Estimates of CO_2 uptake and release among European forests based on eddy covariance data. *Global Change Biol.* **10**, 1445–1459.

Wang, W., Ichii, K., Hashimoto, H., Michaelis, A. R., Thornton, P. E. and co-authors. 2009. A hierarchical analysis of terrestrial ecosystem model Biome-BGC: equilibrium analysis and model calibration. *Ecol. Modell.* **220**, 2009–2023.

Weaver, A. J., Eby, M., Wiebe, E. C., Bitz, C. M., Duffy, P. B. and co-authors. 2001. The UVic Earth System Climate Model: model description, climatology, and applications to past, present and future climates. *Atmos.-Ocean* **39**, 361–428.

Williams, M., Richardson, A. D., Reichstein, M., Stoy, P. C., Peylin, P. and co-authors. 2009. Improving land surface models with FLUXNET data. *Biogeosiences* **6**, 1341–1359.

Wofsy, S. C., Goulden, M. L., Munger, J. W., Fan, S. M., Bakwin, P. S. and co-authors. 1993. Net exchange of CO_2 in a midlatitude forest. *Science* **260**, 1314–1317.

Xiao, J. F., Zhuang, Q. L., Baldocchi, D. D., Law, B. E., Richardson, A. D. and co-authors. 2008. Estimation of net ecosystem carbon exchange for the conterminous United States by combining MODIS and AmeriFlux data. *Agric. Forest Meteorol.* **148**, 1827–1847.

Yang, F. H., Ichii, K., White, M. A., Hashimoto, H., Michaelis, A. R. and co-authors. 2007. Developing a continental-scale measure of gross primary production by combining MODIS and AmeriFlux data through Support Vector Machine approach. *Remote Sens. Environ.* **110**, 109–122.

Yoshikawa, C., Kawamiya, M., Kato, T., Yamanaka, Y. and Matsuno, T. 2008. Geographical distribution of the feedback between future climate change and the carbon cycle. *J. Geophys. Res.-Biogeosci.* **113**, G03002, doi:10.1029/2007JG000570.

Zaehle, S. and Friend, A. D. 2010. Carbon and nitrogen cycle dynamics in the O-CN land surface model: 1. Model description, site-scale evaluation and sensitivity to parameter estimates. *Global Biogeochem. Cycles* **24**, GB1005, doi:10.1029/2009GB003521.

Zaehle, S., Sitch, S., Smith, B. and Hatterman, F. 2005. Effects of parameter uncertainties on the modeling of terrestrial biosphere dynamics. *Global Biogeochem. Cycles* **19**, GB3020, doi:10.1029/2004GB002395.

Zeng, N., Qian, H. F., Munoz, E. and Iacono, R. 2004. How strong is carbon cycle-climate feedback under global warming? *Geophys. Res. Lett.* **31**, L20203, doi:10.1029/2004GL020904.

Zickfeld, K., Eby, M., Matthews, H. D. and Weaver, A. J. 2009. Setting cumulative emissions targets to reduce the risk of dangerous climate change. *Proc. Natl. Acad. Sci. U.S.A.* **106**, 16129–16134.